

Article

All-Fiber Narrow-Bandwidth Mode-Locked Laser Based on Polarization-Dependent Helical Long-Period Grating

Ying Wan ^{1,*}, Chen Jiang ² , Zuxing Zhang ², Yaya Mao ¹, Jianxin Ren ¹, Jianxiang Wen ³ and Yunqi Liu ³

¹ The Jiangsu Key Laboratory for Optoelectronic Detection of Atmosphere and Ocean, School of Physics and Optoelectronic Engineering, Nanjing University of Information Science & Technology, 219 Ningliu Road, Nanjing 210044, China; 002807@nuist.edu.cn (Y.M.); 003458@nuist.edu.cn (J.R.)

² Advanced Photonic Technology Lab, College of Electronic and Optical Engineering & College of Flexible Electronics (Future Technology), Nanjing University of Posts and Telecommunications, 9 Wenyuan Road, Nanjing 210023, China; chenjiang@njupt.edu.cn (C.J.); zxzhang@njupt.edu.cn (Z.Z.)

³ Key Lab of Specialty Fiber Optics and Optical Access Networks, Joint International Research Laboratory of Specialty Fiber Optics and Advanced Communication, School of Communication and Information Engineering, Shanghai University, 99 Shangda Road, Shanghai 200444, China; wenjx@shu.edu.cn (J.W.); yqliu@shu.edu.cn (Y.L.)

* Correspondence: yingwan@nuist.edu.cn

Abstract: As a crucial component of nonlinear polarization rotation (NPR) mode locking, optical fiber gratings offer advantages such as polarization modulation capability, stability, fiber compatibility, and preparation maturity, making them a vital technological foundation for achieving NPR mode locking. Here, a polarization-maintaining fiber helical long-period grating (PMF-HLPG) was designed and fabricated as a polarizer using the CO₂-laser direct-write technique to realize the NPR effect. A homemade fiber Bragg grating (FBG) was also introduced into the laser system to enable a narrow-bandwidth lasing output and wavelength tunability. Based on the PMF-HLPG and FBG mentioned above, an all-fiber mode-locked laser with a spectra bandwidth of 0.15 nm was constructed to generate stable short pulses with a fundamental repetition rate of 12.7122 MHz and a pulse duration of 30.08 ps. In particular, its signal-to-noise ratio is up to 84.5 dB, showing the high stability of the laser. Further, the operating wavelength of the laser can be tuned from 1559.65 nm to 1560.29 nm via heating the FBG while maintaining its mode-locked state with stability. The results indicate that the PMF-HLPG could be used as a polarizer to meet the NPR mechanism for ultrashort pulse laser applications in optical communication, optical sensing, and biomedical imaging.

Keywords: helical long-period fiber grating; polarization-maintaining fiber; nonlinear polarization rotation; mode-locked fiber laser



Citation: Wan, Y.; Jiang, C.; Zhang, Z.; Mao, Y.; Ren, J.; Wen, J.; Liu, Y. All-Fiber Narrow-Bandwidth Mode-Locked Laser Based on Polarization-Dependent Helical Long-Period Grating. *Photonics* **2023**, *10*, 842. <https://doi.org/10.3390/photonics10070842>

Received: 25 June 2023
Revised: 16 July 2023
Accepted: 17 July 2023
Published: 21 July 2023



Copyright: © 2023 by the authors. Licensee MDPI, Basel, Switzerland. This article is an open access article distributed under the terms and conditions of the Creative Commons Attribution (CC BY) license (<https://creativecommons.org/licenses/by/4.0/>).

1. Introduction

With the developed ultrafast fiber laser technology, all-fiber short-pulse mode-locked lasers with a compact structure, good stability, and high beam quality find extensive utility across diverse applications, such as optical biological imaging [1], industrial processing [2], and optical soliton communication [3]. As reported, many saturable absorber (SA) materials, including SESAM [4], graphene [5], carbon nanotubes [6], etc., exhibit a decrease in absorption as the incident optical intensity increases. This non-linear characteristic allows the SA to act as a self-regulating component in a laser cavity, enabling the generation of ultrashort optical pulses. Despite SA materials offering significant advantages, their implementation in fiber lasers is accompanied by certain limitations that affect the output performance due to their low damage threshold and degradation over time. In response to the growing demand for diverse applications, other fiber laser construction based on the optical Kerr effect has been proposed and adopted, including nonlinear optical loop mirrors [7,8], nonlinear amplification loop mirrors [9], nonlinear multimode interference [10],

and nonlinear polarization rotation (NPR) [11,12], etc. Among these options, the NPR mechanism has emerged as a particularly effective and mature approach [13–16]. It is achieved through the collaboration of two polarization controllers (PCs) and polarization-dependent devices. The use of conventional polarization-dependent devices in the NPR mechanism often involves bulky optical polarizers. However, these bulk components pose challenges in terms of miniaturization and integration when it comes to passively mode-locked fiber lasers (MLFLs). In response to the aforementioned challenges, a range of polarization-dependent all-fiber devices have been proposed and developed as a promising alternative. These devices include a segment of polarizing fiber [17], microfiber polarizer [18,19], single-mode-fiber coil [20], fiber grating [12,21–23], and so on. Each of them has its associated advantages and drawbacks. For instance, the polarizing fiber has a high polarization extinction ratio (PER) without any micro-processing; however, it is important to note that the fiber drawing techniques and equipment required for manufacturing polarizing fiber are relatively complex and demanding. Although the microfiber polarizer has the advantages of a low cost and high PER, the microfibers are generally more fragile than regular fibers, which limits their practical application in the laser system. Fiber coils operating in the low-V-number regime can achieve enhanced bend-induced polarization-dependent losses (PDLs) as a polarizer to obtain mode locking. However, it is difficult and uncontrollable to balance the PDL and bending loss of the fiber coils [20]. Compared to the above-mentioned polarizers, fiber gratings demonstrate many advantages. Their wavelength selectivity, design flexibility, all-fiber integration, and compatibility with high-power applications contribute to their versatility and effectiveness in all-fiber laser systems. Mou et al. [21] proposed an all-fiber passively mode-locked laser using a 45° tilted fiber grating (TFG) as an in-fiber polarizer in the laser cavity. Nevertheless, the fabrication of a 45° TFG requires the optical fiber to have strong photosensitivity and demands a high level of precision in the writing system. Then, Huang et al. and Li et al. [12,22] developed MLFLs utilizing a femtosecond laser inscribed in-fiber Brewster device and a small-period long-period grating (LPG), respectively. Nevertheless, complicated femtosecond laser inscription systems are not very affordable and the gratings suffer from a high insertion loss, with values exceeding 7 dB and 15 dB at a wavelength of 1560 nm, respectively. Furthermore, Kanagaraj et al. employed a femtosecond laser to fabricate a 45° TFG with a wavelength of 2 μm, effectively expanding the operating range of mode-locked lasers to the 2 μm waveband. However, it is important to note that the device exhibited significant insertion loss, resulting in a high mode-locking threshold exceeding 300 mW [24], while the polarization-maintaining fiber (PMF) helical LPG (HLPG) could enable effective polarization mode coupling, allowing it to function as an all-fiber polarizer [25]. In comparison to other types of gratings, such as the 45° TFG [21,22], small-period LPG [12], and chiral LPG [23], the PMF-HLPG inscribed by a CO₂-laser offers advantages in terms of simpler and faster manufacturing, a lower insertion loss, and a low cost. Moreover, adopted helical refractive index modulation could also remove the necessity of CO₂-laser exposure alignment along the axis of PMFs during grating inscription, resulting in an improved grating writing efficiency. These merits associated with PMF-HLPG suggest that it could be suitable for applications in NPR MLFLs, which are yet to be exploited.

In this work, we demonstrate the implementation of an all-fiber MLFL utilizing an HLPG within a PMF and a homemade fiber Bragg grating (FBG). The stable narrow bandwidth and tuned wavelength ps pulse lasing were accomplished and the lasing characteristics were systematically investigated in terms of its output spectrum, stability, pulse width, wavelength tunability, and so on.

2. Polarization-Dependent Helical Long-Period Grating and Mode-Locked Fiber Laser Construction

In a conventional single-mode fiber (SMF)-based LPG, the LPG couples the fundamental core mode to various order cladding modes, resulting in a series of resonance dips across a wide range of wavelengths [26]. To enhance the PDL of the grating, two approaches are

commonly employed. The first method involves enhancing the asymmetric refractive index modulation of the grating to introduce birefringence. The second method is to directly fabricate gratings on high-birefringence fibers. Notably, Panda-type PMF is a typical example of a high-birefringence fiber, this fiber achieves higher stress birefringence through the incorporation of a pair of B₂O₃-doped low-refractive-index stress regions in the fiber cladding. As a result of these design features, the PDL can be significantly improved. Therefore, in a PMF, the birefringence and stress-induced anisotropy of the fiber cause the two orthogonal polarization modes to travel at different phase velocities and exhibit different propagation characteristics. This unique property of PMF-based LPGs allows them to couple a pair of orthogonally polarized core fundamental modes to different orders of orthogonally polarized cladding modes [27–29]. Notably, these coupled orthogonally polarized modes exhibit no correlation in wavelength, enabling PMF-based LPGs to effectively function as polarizers [30]. The phase-matching condition of a PMF-based LPG can be described using the coupled mode theory [25,31] as follows:

$$\lambda_i^m = (n_{co,i} - n_{cl,i}^m)\Lambda \quad (1)$$

where λ_i^m represents the resonant wavelength of the m th-order cladding mode in the i polarization direction, and $i = \{x, y\}$ represents the two orthogonal polarized directions of the PMF, corresponding to the fiber slow axis and fast axis, respectively. Λ is the period of the grating and $n_{co,i}$ and $n_{cl,i}$ represent the effective refractive index of the fundamental mode and the m th orthogonally polarized cladding modes, respectively.

A CO₂-laser (CO₂-H10, Han's Laser, Shenzhen, China) was used to inscribe helical refractive index modulation type LPG in a Panda-type PMF (PM 1550 125/13, YOFC). The relative refractive index distribution of the fiber cross-section was measured [25], where the fiber features a core diameter of 8 μm , a cladding diameter of 125 μm , and a stress-applying parts (SAPs) diameter of 32 μm . The centers of the two SAPs are separated by a distance of 54.8 μm . The index difference between the core and cladding is 0.004, while the index difference between the core and SAPs is 0.0164. The helical index modulation in the PMF is achieved by simultaneously rotating the fiber during CO₂-laser irradiation. When inscribing the LPG, one end of the PMF is fixed on a rotating device driven by a step motor, and the other end of the fiber is placed in a fiber slot of the platform so that the fiber can rotate at a constant speed. The pitch of the grating is determined by the combined speed of the fiber's axial movement and rotation. Spiral modulation reduces the writing difficulty of grating in PMF and improves its writing efficiency. Detailed information about other fiber parameters and preparation methods can be found in our previous work [25]. Figure 1 illustrates the schematic diagram of the PMF-HLPG-based polarization-dependent device and polarization spectra measurement system, where the bottom left inset shows the schematic cross-section of the Panda-type PMF and the structure of the PMF-HLPG, respectively. The transmission spectrum of the grating was measured using a broadband light source (BBS, SuperK, NKT Photonics, Copenhagen, Switzerland) and was recorded with an optical spectrum analyzer (OSA, AQ6375, Yokogawa, Tokyo, Japan) with a resolution of 0.05 nm. To optimize the polarization state of the incident light, a polarizer and a PC were placed after the BBS. These components allowed for the precise control and adjustment of the polarization state of the light before interacting with the grating. By adjusting the PC properly, two orthogonal polarization spectra of the PMF-HLPG can be simultaneously output using a polarization beam splitter (PBS), as shown in the right inset picture of Figure 1. According to Equation (1), by designing the grating period, the grating-based polarizer can work in different wavebands. The PMF-HLPG in this experiment was designed with a pitch of 480 μm , and the length of the grating was limited to 2.4 cm. Figure 2a shows the measured two orthogonal polarization transmission spectra (solid lines) and loss spectrum (dotted line) of the PMF-HLPG, where the red and black lines in Figure 2a represent the slow-axis and fast-axis spectra, respectively. The resonant dips observed at 1571.4 nm correspond to the coupling of the fast-axis mode (Y-polar, LP_{15y} mode), while other dips at 1508.6 nm correspond to the coupling of the slow-axis mode (X-polar, LP_{14x} mode) [25]. The dotted line in Figure 2a represents measurements of the

grating under random light input conditions, indicating that the grating has a low insertion loss as a polarizer. As shown in Figure 2b, the PDL spectrum of the PMF-HLPG was measured within the wavelength range of 1540 nm to 1600 nm. The maximum PDL was 26 dB at 1571.4 nm, and its bandwidth greater than 3 dB spanned 24.9 nm, ranging from 1558.8 nm to 1583.7 nm. Importantly, the central wavelength of the PDL spectrum can be adjusted flexibly by modifying the grating period.

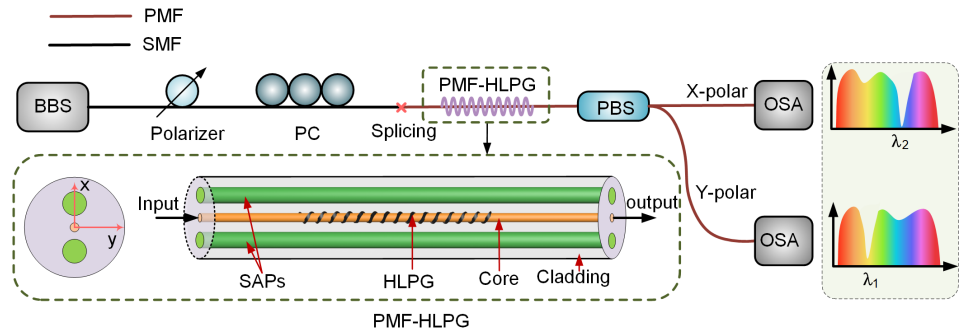


Figure 1. The schematic diagram of the PMF-HLPG-based polarization-dependent device and polarization spectra measurement system, where the bottom-left inset picture shows the schematic cross-section of the Panda-type PMF and the structure of the PMF-HLPG, respectively, and the right inset picture shows the schematic diagram of orthogonal polarization spectra of the PMF-HLPG (BBS: broadband light source, PC: polarization controllers, PMF-HLPG: polarization-maintaining fiber helical long-period grating, PBS: polarization beam splitter, OSA: optical spectrum analyzer, SAPs: stress applying parts).

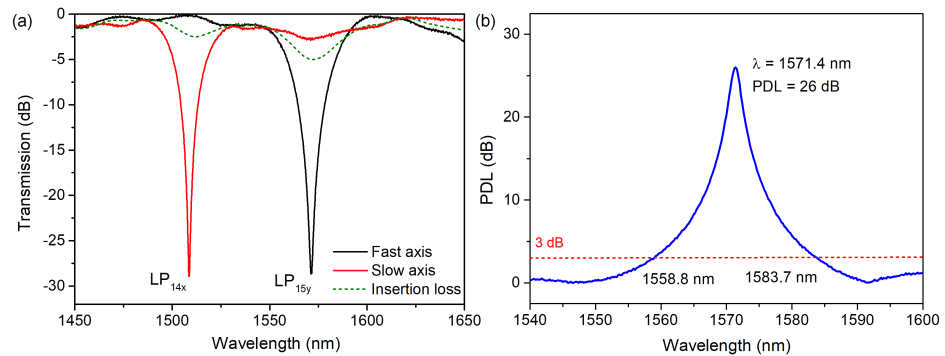


Figure 2. (a) The measured two orthogonal polarization transmission spectra (solid lines) and loss spectrum (dotted line) of the PMF-HLPG with a grating period of 480 μm . (b) The measured PDL spectrum of the PMF-HLPG within the wavelength range of 1540 nm to 1600 nm.

To verify the capability of the PMF-HLPG to function as a polarizer in conjunction with the NPR effect, a ring fiber laser cavity based on the polarization-dependent PMF-HLPG was constructed. Its setup and laser measurement system are illustrated in Figure 3. A single-mode semiconductor laser diode (LD, VLSS-980, Connect, Shanghai, China) operating at a wavelength of 974 nm was used as the pump source. The pump delivers a maximum output power of 500 mW and is coupled into the system through a 980/1550 nm single-mode wavelength division multiplexer (WDM). A piece of 1.0 m commercial erbium-doped fiber (EDF, OFS EDF80) was utilized as the gain media of the laser to provide gain. The 10% port of an optical coupler (OC) served as the laser output, and the 90% light continued to oscillate in the cavity. To obtain a narrow-bandwidth laser output, a homemade FBG was incorporated into the cavity by an optical circulator (CIR) to select mode-locked wavelengths. The transmission spectrum of the FBG is presented in the inset of Figure 3, which can be seen to have a reflectivity of more than 99.0% and 3 dB bandwidths of 0.21 nm at a central wavelength of 1559.39 nm. The CIR in the cavity can also ensure

unidirectional operation in the laser cavity. A 480 μm period PMF-HLPG with fast-axis polarization mode resonance acted as an all-fiber polarizer, which was integrated with two PCs, forming the structure in order to achieve mode locking. The total effective cavity length of the laser is ~ 16.1 m, including 1 m long EDF, ~ 15 m long standard SMF (SMF-28, Corning, New York, NY, USA), and 0.1 m long PMF, which entails a fundamental repetition rate of 12.76 MHz. The group velocity dispersions of the EDF and SMF are 61.15 ps^2/km and -22.8 ps^2/km at wavelength 1550 nm, respectively, and the dispersion of the 0.1 m PMF was ignored in this experiment, so the total net cavity dispersion of the laser was calculated to be approximately -0.283 ps^2 . The output properties of the MLFL, including spectrum, pulse train, RF spectrum, and autocorrelation trace, were measured, depending on an OSA (AQ6370D, Yokogawa, Tokyo, Japan), an oscilloscope (DS4050, RIGOL, Wuhan, China) with a 10 GHz photodetector (PD, 818-BB-51F, Newport, Irvine, CA, USA), an electrical spectrum analyzer (ESA, RS-FSV3000, Rohde & Schwarz, Munich, Germany), and an autocorrelator (PulseCheck SM1600, APE, Berlin, Germany), respectively.

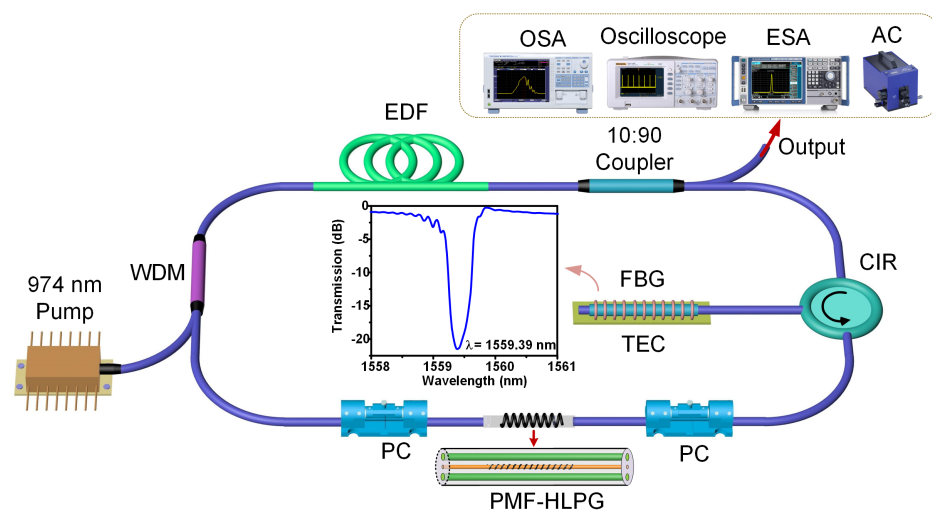


Figure 3. Setup of narrow bandwidth MLFL based on PMF-HLPG and FBG, and the laser measurement system (WDM: wavelength division multiplexer, EDF: erbium-doped fiber, CIR: optical circulator, FBG: fiber Bragg grating, TEC: temperature electric controller). The inset is the transmission spectra of the FBG.

3. Evaluation of the Narrow Bandwidth and Wavelength-Tunable Mode-Locked Fiber Laser

A stable anomalous dispersion MLFL was accomplished by slightly adjusting the PCs and the pump power. The mode-locked threshold of the laser is approximately 110 mW. In comparison to other grating-based polarization devices [12,22], the PMF-HLPG-based laser exhibits a lower mode-locking threshold. By reducing the loss of the other device in the cavity, the mode-locking threshold of the laser can be further reduced. Its output characteristics were analyzed at a pump power of 120 mW, in terms of the optical spectrum, pulse train, RF spectrum, and autocorrelation trace. As shown at the top of Figure 4a, the output spectrum of the laser was scrutinized using an OSA with a resolution of 0.02 nm. And a narrow-bandwidth lasing peak centered at 1559.65 nm can be observed, associated with a narrow bandwidth of 0.15 nm at 3 dB. At the same time, there are three visible Kelly sideband peaks on the right side of the spectrum, which proves that the fiber laser works in a conventional soliton regime. The narrow bandwidth profile of the laser depends mainly on the property of the FBG within the laser cavity, suggesting that the bandwidth of the laser spectrum can further be compressed by using a smaller-bandwidth FBG [32]. The power stability of the mode-locked fiber laser under a pump power of 120 mW was successively measured using a power meter, every 1 s for 2 h. The result is shown in the inset of Figure 4a. The fluctuation in the output power (FOP) is less than 0.02% of the

average power (output power: 1.967 mW), which is indicative of stable output power. The spectral stability of the laser was continuously monitored for every 5 min over 4 h as depicted at the bottom of Figure 4a. The central wavelength fluctuation is less than 0.01 nm, and the intensity fluctuation is lower than 0.01% of the average spectral intensity at 1559.65 nm. This suggests that no obvious spectral changes are observed, suggesting that the laser exhibits a well-stabilized mode-locked state. The illustration in Figure 4b shows the pulse train of the fiber laser, which was detected by an oscilloscope with a 10 GHz PD. The pulse train over the time scale of 7 μ s was recorded. The intensity fluctuation of the pulse train is less than 0.08% of the average voltage, which is attributed to the low resolution of the oscilloscope. By the enlarged pulse train, the pulse interval time was evaluated to be 78.66 ns, corresponding to the calculated pulse repetition rate of 12.7122 MHz, which matches well with the cavity length. The radio frequency (RF) spectrum with a single peak at 12.7122 MHz was recorded via an ESA with a resolution of 1 Hz, as demonstrated in Figure 4c. In other words, the fundamental repetition rate of the laser is 12.7122 MHz, which is in agreement with the calculated pulse repetition rate and laser cavity length of 16.1 m. It is worth noting that, during the experiments, we observed a stable harmonic mode-locking state of the laser by increasing the pump power and appropriately adjusting the polarization state within the cavity. However, controlling the order of the harmonic mode-locking pulse trains is still a challenge. An 84.5 dB signal-to-noise ratio (SNR) and a narrow spectral width demonstrate excellent pulse energy stability and low pulse timing jitter. In the inset of Figure 4c, the RF spectrum of the fundamental repetition rate and its beat note is monitored over a 1 GHz frequency range with a 10 kHz resolution bandwidth, implicating a stable mode-locked operation obtained in the fiber laser. In addition, the autocorrelation trace of the mode-locked pulses was measured using an autocorrelator with a measuring range of 120 ps, and the result is shown in Figure 4d. A broadband peak was recorded and fitted with the sech^2 curve, indicating a full width at half maximum (FWHM) of 46.408 ps and a pulse duration of 30.08 ps for the MLFL. Therefore, the calculated time–bandwidth product (TBP) is 0.5564, which is larger than the Fourier transform limit of the hyperbolic secant pulse (0.3), implying that this sech^2 pulse still possesses chirp. This means that the pulses can be compressed further in the time domain, which has the potential to be developed and optimized in the future. The above results confirm that the MLFL based on PMF-HLPG and FBG is a narrow-bandwidth and high-stability picosecond pulse fiber laser.

In addition, the tunable performance of the MLFL based on PMF-HLPG and FBG was demonstrated by the temperature sensitivity of the FBG. As the temperature of the FBG was gradually increased from 25 °C to 95 °C, the central wavelength of the laser was red-shifted and the spectral profile remained unchanged, as illustrated in Figure 5a. Note that both the PCs and the output power of the pump laser in the laser system remain unchanged during the temperature adjustment process, i.e., the mode-locked state of the laser remains unchanged. As shown in Figure 5b, a lasing central wavelength tuning range of approximately 0.64 nm was accomplished from 1559.65 nm to 1560.29 nm. The wavelength shift increases linearly with the temperature at a slope coefficient of 9.40 pm/°C. The operating wavelength of the MLFL based on PMF-HLPG was tuned by temperature, demonstrating that the laser has the ability to be tuned. At the same time, the laser remained in a stable state during the wavelength tuning process, indicating that the PMF-HLPG has a good mode-locked performance. To enhance the wavelength tunable range, further optimization can be pursued through methods like enhancing the temperature sensitivity of the FBG or utilizing the tensile or bending sensitivity of the FBG. These approaches offer potential avenues for expanding the range of the lasing working wavelength. Meanwhile, the temporal pulse train and autocorrelation trace of the laser at different operating wavelengths were measured, and the results at three typical wavelengths are presented in Figure 5c,e, respectively. The fluctuations of the laser output characteristics are summarized in Figure 5d,f. As the working wavelength red-shifts, the pulse interval time increases slightly, i.e., from 78.6646 ns to 78.6658 ns; thus, the repetition

frequency decreases from 12.7122 MHz to 12.7120 MHz. The fluctuations in bandwidth and pulse width are less than 0.013 nm and 5 ps, respectively, which results in small fluctuations in the TBP of the laser as well (less than 0.13). Those small fluctuations are mainly caused by the differences in gain and loss in the cavity at different operating wavelengths, as well as a small variation in cavity length caused by changes in the effective length of the FBG at different temperatures. The results indicate that the MLFL based on PMF-HLPG exhibits a stable wavelength tuning capability.

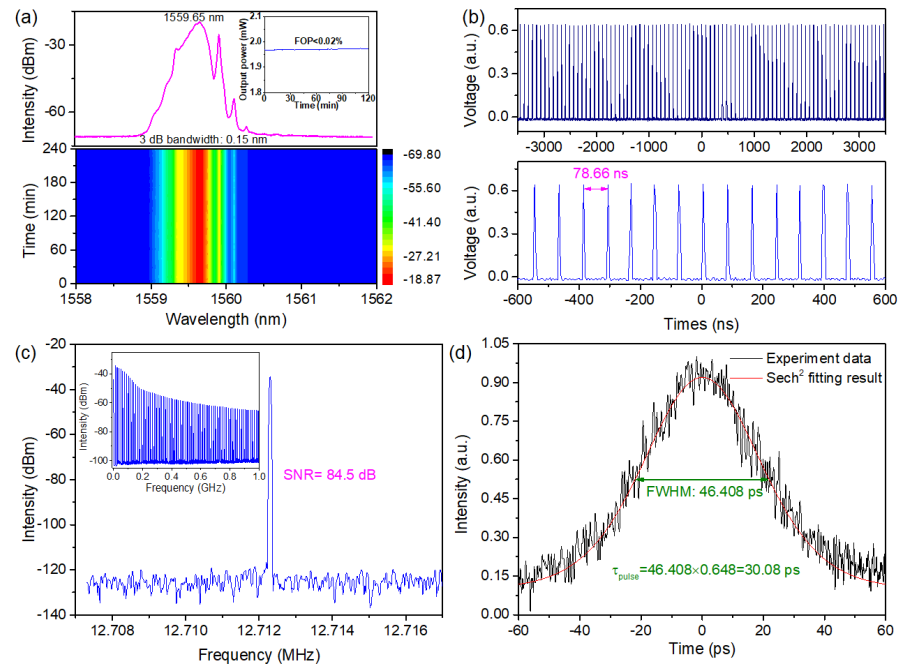


Figure 4. The output characteristics of the narrow bandwidth MLFL at a pump power of 120 mW. (a) Output spectrum with 0.02 nm resolution and its stability over 4 h. The inset is laser output power stability with 2 h at 1.967 mW. (b) The temporal pulse train at different ranges. (c) RF spectrum with 10 kHz span and 1 Hz resolution bandwidth, and the inset shows the RF spectrum in a 1 GHz range with 10 kHz resolution bandwidth. (d) Autocorrelation trace with the sech² fitting.

Utilizing a PMF-HLPG as an in-fiber polarizer in MLFL provides several significant advantages compared to MLFL, which relies on commercial bulk polarizers, including a lower insertion loss, all-fiber structure with higher integration, and lower cost. Moreover, compared to other all-fiber polarization-dependent devices, the PMF-HLPG also exhibits an excellent performance. According to the above experimental results, it can be found that the PMF-HLPG has three obvious advantages as an all-fiber polarizer to realize mode locking. Firstly, the fabrication method of the PMF-HLPG is simple and has a low cost. The PMF-HLPG was fabricated using the CO₂-laser writing technique, which has a high writing efficiency and stability [25,33]. Compared with the femtosecond laser-inscribed grating system and UV laser-written grating system, this approach eliminates the need for expensive laser inscription systems and fiber pretreatment, facilitating the design of in-fiber polarization-dependent devices. Secondly, it has a wide operating bandwidth and wavelength selectivity. In this work, the PMF-HLPG succeeded in achieving a stable mode-locked laser output with a PDL of only 3.5 dB, indicating an operating bandwidth of at least 20 nm for the fast axis and a similar effect for the slow axis, rendering the device highly suitable as a polarizer within the C+L band. By inscribing phase-shifting HLPG, a cascading grating, and a dispersion turning point grating on PMFs, the working bandwidth of the polarizer can be effectively expanded. These methods enable further enhancements in the operational wavelength range of the PMF-HLPG-based polarizer. Moreover, the working wavelength of the grating can be flexibly adjusted by altering the period of the

PMF-HLPG. This adaptability allows the grating to be utilized in the construction of MLFLs operating at different wavebands, such as a 1.0-, 1.55-, and 2.0- μm waveband. It should be noted here that the effect of the magnitude of the PDL on the mode-locked characteristics of the laser still needs further systematic investigation. Thirdly, the MLFL built based on PMF-HLPG has a good stability and high SNR. This is mainly dependent on the stable polarization modulation characteristics of the PMF-HLPG. Therefore, the work presented here provides a novel and alternative method for implementing a mode-locked laser output, and could also shed light on the study of stable NPR-based ultrashort pulse fiber lasers across various operating wavelengths.

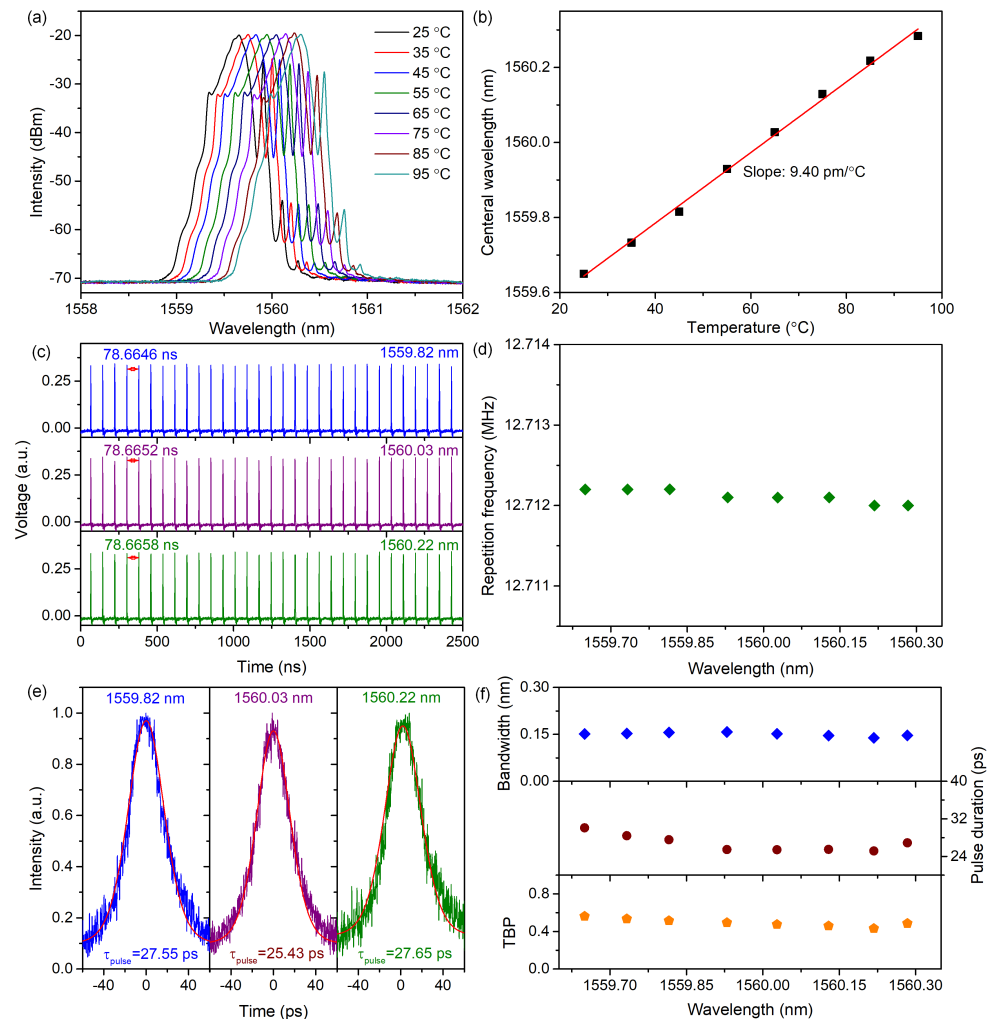


Figure 5. The output characteristics of the MLFL based on an FBG at different working temperatures. (a) Optical spectrum at different working wavelengths. (b) Laser wavelength versus different temperatures of the FBG. (c) The temporal pulse train and (d) autocorrelation trace of the laser at three operating wavelengths. (e) The repetition frequency and (f) bandwidth (blue square), pulse duration (dark red circle), and TBP (orange circle) variations of different working wavelengths.

4. Conclusions

In conclusion, we designed and fabricated a PMF-HLPG using the CO₂-laser writing technique to meet the requirements of the NPR mechanism and a homemade FBG with 3 dB bandwidths of 0.21 nm to obtain narrow-bandwidth lasing and wavelength tuning. A stable 0.15 nm bandwidth mode-locked ps pulse lasing with an SNR of 84.5 dB was demonstrated in an NPR MLFL based on a PMF-HLPG and an FBG. To the best of our knowledge, it is the first time that the PMF-HLPG has been utilized as a polarizer to implement narrow-bandwidth MLFLs. In addition, the laser exhibits the ability to be continuously tuned

within the range of 1559.65 nm to 1560.29 nm while also maintaining the stability of its mode-locked state. The study results indicate that the NPR structure, utilizing the PMF-HLPG, can provide valuable insights for the exploration of compact, stable, and robust all-fiber ultrafast lasers in practical applications across various operating wavelengths. Future research may aim to enhance the tunable range of this narrow-bandwidth mode-locked laser and investigate the impact of PDL variation at different wavelengths in the PMF-HLPG on the laser output characteristics. By addressing these aspects, we aim to further enhance the overall performance of the laser.

Author Contributions: Conceptualization, Y.W., C.J., Z.Z. and Y.L.; methodology, Y.W., C.J. and Z.Z.; validation, Y.W. and C.J.; investigation, Y.W. and C.J.; resources, Z.Z., Y.M. and J.R.; writing—original draft preparation, Y.W.; writing—review and editing, Y.W. and C.J.; project administration, Y.W., C.J., J.W. and Y.L. All authors have read and agreed to the published version of the manuscript.

Funding: This work is supported by the Startup Foundation for Introducing Talent of NUIST, Basic Science (Natural Science) Research Program of Higher Education Institutions in Jiangsu Province (23KJB140014), Natural Science Research Start-up Foundation of Recruiting Talents of Nanjing University of Posts and Telecommunications (NY223035), and the National Science Foundation of China under Grants (62075124, 61705126).

Institutional Review Board Statement: Not applicable.

Informed Consent Statement: Not applicable.

Data Availability Statement: Data underlying the results presented in this paper are not publicly available at this time but may be obtained from the authors upon reasonable request.

Conflicts of Interest: The authors declare no conflict of interest.

References

1. Xu, C.; Wise, F. Recent advances in fibre lasers for nonlinear microscopy. *Nat. Photonics* **2013**, *7*, 875–882. [[CrossRef](#)] [[PubMed](#)]
2. Bogusławski, J.; Soboń, G.; Zybala, R.; Sotor, J. Towards an optimum saturable absorber for the multi-gigahertz harmonic mode locking of fiber lasers. *Photonics Res.* **2019**, *7*, 1094–1100. [[CrossRef](#)]
3. Hasegawa, A. Soliton-based optical communications: An overview. *IEEE J. Sel. Top. Quantum Electron.* **2000**, *6*, 1161–1172. [[CrossRef](#)]
4. Tang, G.; Qian, G.; Lin, W.; Wang, W.; Shi, Z.; Yang, Y.; Dai, N.; Qian, Q.; Yang, Z. Broadband 2 μm amplified spontaneous emission of Ho/Cr/Tm: YAG crystal derived all-glass fibers for mode-locked fiber laser applications. *Opt. Lett.* **2019**, *44*, 3290–3293. [[CrossRef](#)]
5. Martinez, A.; Sun, Z. Nanotube and graphene saturable absorbers for fibre lasers. *Nat. Photonics* **2013**, *7*, 842–845. [[CrossRef](#)]
6. Huang, L.; Zhang, Y.; Liu, X. Dynamics of carbon nanotube-based mode-locking fiber lasers. *Nanophotonics* **2020**, *9*, 2731–2761. [[CrossRef](#)]
7. Malfondet, A.; Parriaux, A.; Krupa, K.; Millot, G.; Tchofo-Dinda, P. Optimum design of NOLM-driven mode-locked fiber lasers. *Opt. Lett.* **2021**, *46*, 1289–1292. [[CrossRef](#)]
8. Ma, X.; Lv, J.; Luo, J.; Liu, X.; Yao, P.; Xu, L. Pulse convergence analysis and pulse information calculation of NOLM fiber mode-locked lasers based on machine learning method. *Opt. Laser Technol.* **2023**, *163*, 109390. [[CrossRef](#)]
9. Kim, D.; Kwon, D.; Lee, B.; Kim, J. Polarization-maintaining nonlinear-amplifying-loop-mirror mode-locked fiber laser based on a 3×3 coupler. *Opt. Lett.* **2019**, *44*, 1068–1071. [[CrossRef](#)]
10. Chen, T.; Zhang, Q.; Zhang, Y.; Li, X.; Zhang, H.; Xia, W. All-fiber passively mode-locked laser using nonlinear multimode interference of step-index multimode fiber. *Photonics Res.* **2018**, *6*, 1033–1039. [[CrossRef](#)]
11. Alamgir, I.; Rochette, M. Thulium-doped fiber laser mode-locked by nonlinear polarization rotation in a chalcogenide tapered fiber. *Opt. Express* **2022**, *30*, 14300–14310. [[CrossRef](#)] [[PubMed](#)]
12. Li, Q.; Cheng, P.; Zhao, R.; Cai, J.; Shen, M.; Shu, X. Mode-locked fiber laser based on a small-period long-period fiber grating inscribed by femtosecond laser. *Opt. Lett.* **2023**, *48*, 2241–2244. [[CrossRef](#)] [[PubMed](#)]
13. Peng, J.; Boscolo, S.; Zhao, Z.; Zeng, H. Breathing dissipative solitons in mode-locked fiber lasers. *Sci. Adv.* **2019**, *5*, eaax1110. [[CrossRef](#)]
14. Guo, Y.; Liu, Y.g.; Wang, Z.; Wang, Z.; Zhang, H. All-fiber mode-locked cylindrical vector beam laser using broadband long period grating. *Laser Phys. Lett.* **2018**, *15*, 085108. [[CrossRef](#)]
15. Wang, S.; Zhao, Z.; Kobayashi, Y. Wavelength-spacing controllable, dual-wavelength synchronously mode locked Er: Fiber laser oscillator based on dual-branch nonlinear polarization rotation technique. *Opt. Express* **2016**, *24*, 28228–28238. [[CrossRef](#)] [[PubMed](#)]

16. Wang, Z.; Zhan, L.; Fang, X.; Gao, C.; Qian, K. Generation of sub-60 fs similaritons at 1.6 μm from an all-fiber Er-doped laser. *J. Light. Technol.* **2016**, *34*, 4128–4134. [[CrossRef](#)]
17. Panasencko, D.; Polynkin, P.; Polynkin, A.; Moloney, J.V.; Mansuripur, M.; Peyghambarian, N. Er-Yb femtosecond ring fiber oscillator with 1.1-W average power and GHz repetition rates. *IEEE Photonics Technol. Lett.* **2006**, *18*, 853–855. [[CrossRef](#)]
18. Zhang, Z.; Gan, J.; Yang, T.; Wu, Y.; Li, Q.; Xu, S.; Yang, Z. All-fiber mode-locked laser based on microfiber polarizer. *Opt. Lett.* **2015**, *40*, 784–787. [[CrossRef](#)]
19. Zhou, X.; Qiu, M.; Qian, Y.; Chen, M.; Zhang, Z.; Zhang, L. Microfiber-based polarization beam splitter and its application for passively mode-locked all-fiber laser. *IEEE J. Sel. Top. Quantum Electron.* **2020**, *27*, 0900206. [[CrossRef](#)]
20. Jiang, H.; Huang, Y.; Zhao, Z.; Shirahata, T.; Jin, L.; Yamashita, S.; Set, S.Y. Laser mode locking using a single-mode-fiber coil with enhanced polarization-dependent loss. *Opt. Lett.* **2020**, *45*, 2866–2869. [[CrossRef](#)]
21. Mou, C.; Wang, H.; Bale, B.G.; Zhou, K.; Zhang, L.; Bennion, I. All-fiber passively mode-locked femtosecond laser using a 45°-tilted fiber grating polarization element. *Opt. Express* **2010**, *18*, 18906–18911. [[CrossRef](#)] [[PubMed](#)]
22. Huang, Z.; Huang, Q.; Theodosiou, A.; Cheng, X.; Zou, C.; Dai, L.; Kalli, K.; Mou, C. All-fiber passively mode-locked ultrafast laser based on a femtosecond-laser-inscribed in-fiber Brewster device. *Opt. Lett.* **2019**, *44*, 5177–5180. [[CrossRef](#)] [[PubMed](#)]
23. Du, Y.; Shu, X.; Xu, Z. All-fiber passively mode-locked laser based on a chiral fiber grating. *Opt. Lett.* **2016**, *41*, 360–363. [[CrossRef](#)] [[PubMed](#)]
24. Kanagaraj, N.; Theodosiou, A.; Aubrecht, J.; Peterka, P.; Kamradek, M.; Kalli, K.; Kasik, I.; Honzatko, P. All fiber mode-locked thulium-doped fiber laser using a novel femtosecond-laser-inscribed 45°-plane-by-plane-tilted fiber grating. *Laser Phys. Lett.* **2019**, *16*, 095104. [[CrossRef](#)]
25. Jiang, C.; Liu, Y.; Zhao, Y.; Mou, C.; Wang, T. Helical long-period gratings inscribed in polarization-maintaining fibers by CO₂ laser. *J. Light. Technol.* **2018**, *37*, 889–896. [[CrossRef](#)]
26. Shu, X.; Zhang, L.; Bennion, I. Sensitivity characteristics of long-period fiber gratings. *J. Light. Technol.* **2002**, *20*, 255.
27. Iadicicco, A.; Ranjan, R.; Esposito, F.; Campopiano, S. Arc-induced long period gratings in polarization-maintaining panda fiber. *IEEE Photonics Technol. Lett.* **2017**, *29*, 1533–1536. [[CrossRef](#)]
28. Jiang, C.; Liu, Y.; Mou, C. Polarization-maintaining fiber long-period grating based vector curvature sensor. *IEEE Photonics Technol. Lett.* **2021**, *33*, 358–361. [[CrossRef](#)]
29. Jiang, C.; Liu, Y.; Wan, Y.; Lin, Y.; Mou, C.; Ma, Y.; Zhou, K. Broadband and stable linearly polarized mode converter based on polarization-maintaining fiber long-period grating. *Opt. Laser Technol.* **2022**, *152*, 108159. [[CrossRef](#)]
30. Ortega, B.; Dong, L.; Liu, W.; De Sandro, J.; Reekie, L.; Tsypina, S.; Bagratashvili, V.; Laming, R. High-performance optical fiber polarizers based on long-period gratings in birefringent optical fibers. *IEEE Photonics Technol. Lett.* **1997**, *9*, 1370–1372. [[CrossRef](#)]
31. Noda, J.; Okamoto, K.; Sasaki, Y. Polarization-maintaining fibers and their applications. *J. Light. Technol.* **1986**, *4*, 1071–1089. [[CrossRef](#)]
32. Li, W.; Huang, Z.; Xiao, X.; Yan, Z.; Luo, S.; Song, Y.; Jiang, C.; Liu, Y.; Mou, C. 0.017 nm, 143 ps passively mode-locked fiber laser based on nonlinear polarization rotation. *Opt. Lett.* **2023**, *48*, 2676–2679. [[CrossRef](#)] [[PubMed](#)]
33. Liu, Y.; Lee, H.W.; Chiang, K.S.; Zhu, T.; Rao, Y.J. Glass Structure Changes in CO₂-Laser Writing of Long-Period Fiber Gratings in Boron-Doped Single-Mode Fibers. *J. Light. Technol.* **2009**, *27*, 857–863. [[CrossRef](#)]

Disclaimer/Publisher’s Note: The statements, opinions and data contained in all publications are solely those of the individual author(s) and contributor(s) and not of MDPI and/or the editor(s). MDPI and/or the editor(s) disclaim responsibility for any injury to people or property resulting from any ideas, methods, instructions or products referred to in the content.